NURETH14-145

A CFD BENCHMARKING EXERCISE BASED ON FLOW MIXING IN A T-JUNCTION

B. L. Smith¹, J. H. Mahaffy² and K. Angele³¹ Paul Scherrer Institute, Villigen PSI, Switzerland
² Wheelsmith Farm, Spring Mill, PA A, USA
³ Vattenfall R&D, Älvkarleby, Sweden

Abstract

The paper describes an international benchmarking exercise, sponsored by the OECD Nuclear Energy Agency, aimed at testing the ability of state-of-the-art Computational Fluid Dynamics (CFD) codes to predict the important flow parameters affecting high-cycle thermal fatigue induced by turbulent mixing in T-junctions. Numerical simulations were compared against measured data from an experiment performed at 1:2 scale by Vattenfall Research and Development, Älvkarleby, Sweden. The test data were released only at the end of the exercise. Details of the organizational procedures, the experimental set-up and instrumentation, the different modeling approaches adopted, synthesis of results and overall conclusions and perspectives are presented.

Introduction

As part of an ongoing commitment to extend the assessment database for the application of CFD to nuclear reactor safety issues, a *Special CFD Group* has been formed within the scope of activities of the OECD/NEA[#] Working Group on the Analysis and Management of Accidents (WGAMA) with a mandate to encourage nuclear departments at universities and research institutes to release test data to be used as the basis for international numerical benchmarking exercises. The first such exercise was launched in 2009, and was aimed at testing the ability of state-of-the-art CFD codes to predict the important flow parameters affecting high-cycle thermal fatigue in pipework induced by turbulent mixing in a T-junction.

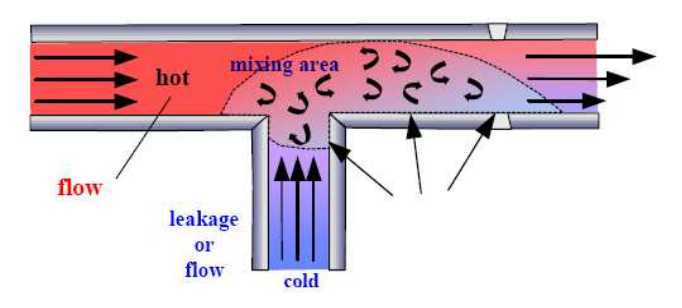


Figure 1. Schematic of turbulent mixing in a T-junction

In T-junctions, where hot and cold streams mix (Fig. 1), significant temperature fluctuations can be created near the walls. The induced wall temperature oscillations can cause cyclical thermal stresses

[#] Organisation for Economic Cooperation and Development, Nuclear Energy Agency

which may lead to fatigue cracking. Thermal striping and the related fatigue problem was initially studied in the context of Liquid-Metal Fast Breeder Reactors (LMFBRs) in the 1980's, when thermal fatigue phenomena had been observed in the secondary loop of the French Phénix prototype LMFBR, as well as in a T-junction of the full-scale Superphénix reactor. The IAEA[%] organised a benchmark activity to study these events, and subsequently issued a document on the subject [1].

The issue of thermal fatigue has since shifted to Light Water Reactors (LWRs), for which several incidents of high-cycle fatigue had been observed, mainly in T-junctions, such as the failure event at Civaux-1 in France in 1998 [2,3]. The incident has also raised thermal fatigue to being of serious safety concern, and an important aspect in regard to ageing and life-management of LWRs. The coolant temperature oscillations are due to turbulent thermal-mixing effects and/or low-frequency flow instabilities [3], with most risk of wall thermal fatigue being reported to be caused by frequencies up to several Hz [4]. Significantly higher frequencies than these appear not to be of concern, as they are strongly attenuated by the thermal inertia of the pipe material. Recent research activity includes a joint US-Japanese programme [5,6,7], a programme by EDF [8], the experiments and benchmarks undertaken by Vattenfall [9,10] and the comprehensive European 5th Framework Programme THERFAT [11], each addressing different aspects of the issue: i.e. thermal-hydraulic analysis, material stress/fatigue analysis, crack initiation and propagation assessment.

Interest in thermal mixing in T-junctions appears to be widespread, and experiments have been carried out in France, Germany, Japan, Sweden and Switzerland. In particular, very careful experiments have been performed since 2006 at the Älvkarleby Laboratory of Vattenfall Research and Development in Sweden, with the specific aim of providing high-quality validation data for CFD simulations. Tests were performed for a variety of main/branch flowrate ratios, and previously unreleased data from one of these tests provided the basis for the benchmark exercise reported here.

1. Organisational Aspects

An organising committee was formed comprising members of the *Special CFD Group*, together with the Vattenfall R&D staff member who carried out the T-junction experiment in 2008. Table 1 lists the members of the committee, their affiliations, and their principal functions within the scope of the benchmark exercise. A date was fixed for a kick-off meeting for the benchmark exercise (20 May, 2009). An announcement was prepared, with an invitation to register interest in receiving the benchmark specifications. Of the 750 or so recipients of this invitation, 65 registrations were received from organisations in 22 countries, of whom 28 attended the kick-off meeting.

Table 1. Members of the Organising Committee and their Principal Functions

Brian L. Smith	PSI, Switzerland	Chairman
Kristian Angele	Vattenfall R&D, Sweden	Performed T-junction experiment
John H. Mahaffy	PSU (Emeritus), USA	Performed synthesis of results
Ghani Zigh	US NRC, USA	Chair: CFD4NRS-3 workshop
Dominique Bestion	CEA, France	Special advisor
Jong-Chul Jo	OECD/NEA, France	Secretariat

[%] International Atomic Energy Agency

The timetable for the benchmark activity is given in Table 2. A draft version of the specifications was circulated to all registered participants on June 30, 2009 with an invitation for feedback concerning errors, clarity, ambiguity and possible misunderstandings. With very few changes, the final and official version was circulated on July 15, 2009. This gave participants 9½ months to complete their calculations and submit their results by the deadline date of April 30, 2010. In total, 29 were received by this date. These form the basis of the synthesis described below.

Table 2. Timetable for the OECD/NEA-Vattenfall T-Junction Benchmark

May 20, 2009	Kick-Off Meeting
June 10, 2009	Distribution of draft version of the Benchmark Specifications
June 30, 2009	Deadline for comment/queries from participants concerning the Benchmark Specifications
July 15, 2009	Distribution of final version of the Benchmark Specifications
April 30, 2010	Deadline for receipt of simulation results
May 12, 2010	Open Benchmark Meeting (first release of test data)
Sept. 14, 2010	Presentation of Results and Synthesis at CFD4NRS-3 Workshop

2. Experiment

2.1 General Layout

The model of the T-junction is manufactured in Plexiglas® and consists of a horizontal pipe with inner diameter (D_2) 140 mm for the cold water flow (Q_2), and a vertically oriented pipe with inner diameter (D_1) 100 mm for the hot water flow (Q_1). The hot water pipe is attached to the upper side of the horizontal cold water pipe. The junction itself is constructed from a solid Plexiglas® block into which the main and branch pipes fit. The test rig is illustrated in Fig. 2.

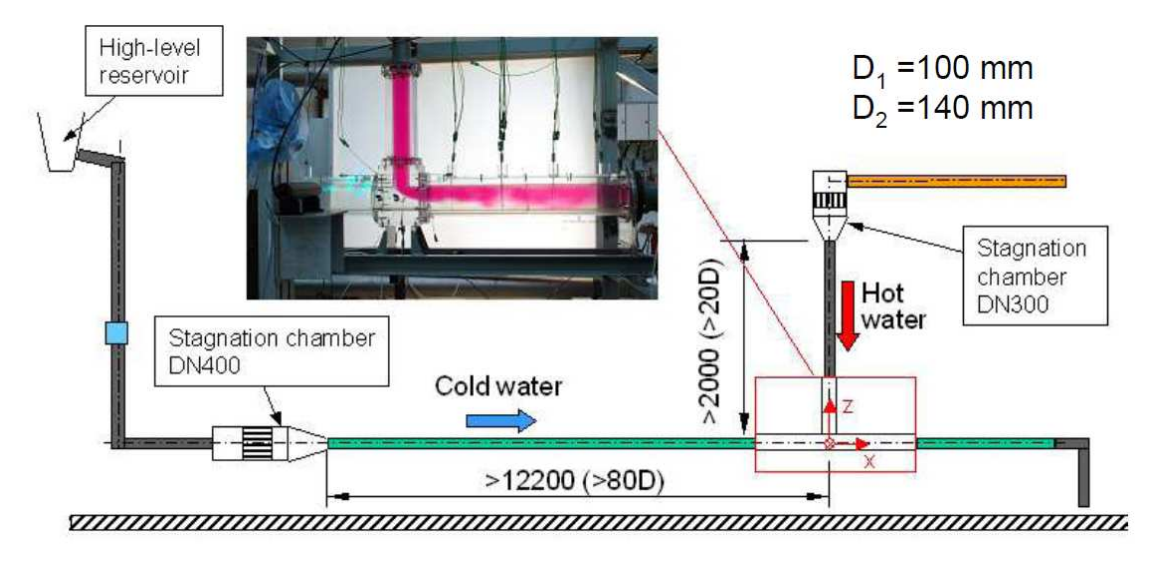


Figure 2. Side view of Vattenfall T-junction test rig

The cold water pipe is supplied from a high-level reservoir equipped with a long horizontal weir to keep a constant water level independently of the flowrate through the model. The flowrate is measured using an electro-magnetic flow meter (blue square in Fig. 2). A stagnation chamber of diameter 400 mm is mounted at the beginning of the horizontal pipe, and contains two perforated plates, a tube bundle (inner diameter of the tubes is 10 mm and the length is 150 mm), a third perforated plate, and finally a contraction, with area ratio 8.2:1. The purpose of the stagnation chamber is to provide a high flow quality without large-scale turbulence or secondary flows. The stagnation chamber is connected to a 10 m long pipe section made from ABS plastic, which is followed by the Plexiglas® section extending 1260 mm upstream of the T-junction. The total upstream length of the pipe with constant diameter ($D_2 = 140 \text{ mm}$) is then more than 80 hydraulic diameters, thus ensuring fully developed flow conditions at the entrance to the junction.

The hot water is taken from a $80 \, \text{m}^3$ reservoir, and a pump is used to feed the test section. The rotational speed of the pump is automatically controlled to maintain a constant flowrate. The stagnation chamber (diameter $300 \, \text{mm}$) is similar to that on the cold-water leg except that the water supply is from the side via a flow distributor. The stagnation chamber is connected to a steel pipe with inner diameter $100 \, \text{mm}$, thus giving an area contraction ratio of 9:1. The total distance with constant diameter ($D_1 = 100 \, \text{mm}$) upstream of the T-junction is approximately $20 \, \text{hydraulic}$ diameters. Fully developed pipe flow conditions cannot be achieved in this case, but the flow quality will be good.

2.2 Instrumentation

Velocity profiles upstream were measured for each inlet pipe using a two-component Laser Doppler Velocimetry (LDV) system, and Particle Imaging Velocimetry was used in cross-sections located at $x/D_2 = 1.6$, 2.6, 3.6 and 4.6 downstream of the T-junction (see Fig. 3). The velocity measurements were performed under cold conditions to avoid distortions due to the change in the refractive index of the water with temperature. The test was then repeated under (mildly) hot conditions (temperature difference 15-20 K) for the thermocouple (TC) measurements. Full details of the LDV/PIV systems are given in separate papers [12,13].

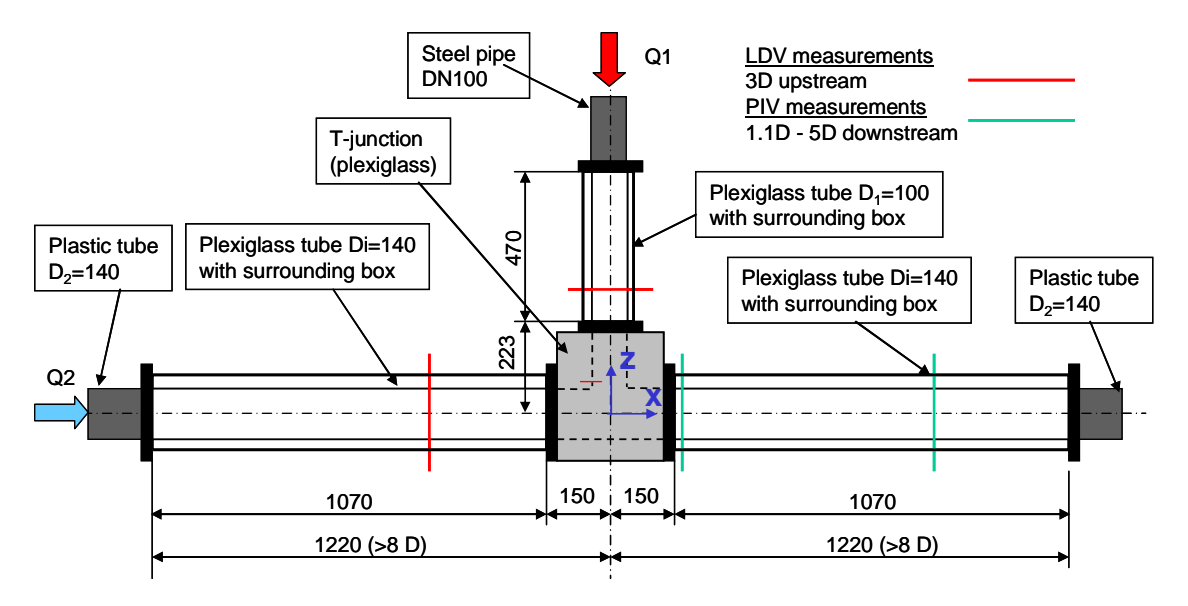


Figure 3. T-junction test section showing LDV and PIV measurement stations

The inlet mean velocity and turbulence profiles in the horizontal pipe were checked against other experimental data for fully developed pipe flow at similar Reynolds numbers [14] and found to be in good agreement with them. The flow is not fully developed in the vertical pipe. The uncertainty in the LDV data is divided into random and systematic errors. The total random uncertainty, normalized with the bulk velocity, is within 2-3% for the streamwise mean velocity and 3-4% for its root-mean-square (rms) value. Systematic errors mainly derive from positioning errors for the LDV system. The global uncertainty in the LDV measurements is estimated to be between 6-8% for the different quantities. The discrepancy between the flowrate calculated on the basis of the integrated LDV data and that measured by the flow meter was approximately 5% [12].

The statistical errors in the PIV data were shown to be below 1% for both the mean and rms values. As a sensitivity check, the data at one measuring location was evaluated with two different software packages (based on different algorithms), and with slightly different settings, displaying differences of 1.7% (on average) in the mean velocity and up to 4% locally. If the different estimations for the relative errors are conservatively added as independent errors, this leads to a total relative error of the order of 5% in the mean velocity. In addition, the absolute error for the uncertainty in the subpixel interpolation (corresponding to about 0.02 m/s) must also be added. The errors in the rms values are roughly double this due to error propagation. The above uncertainty holds primarily in the bulk of the flow and for the streamwise component for which the time delay is optimized. Closer to the walls the uncertainty increases and is also more difficult to estimate.

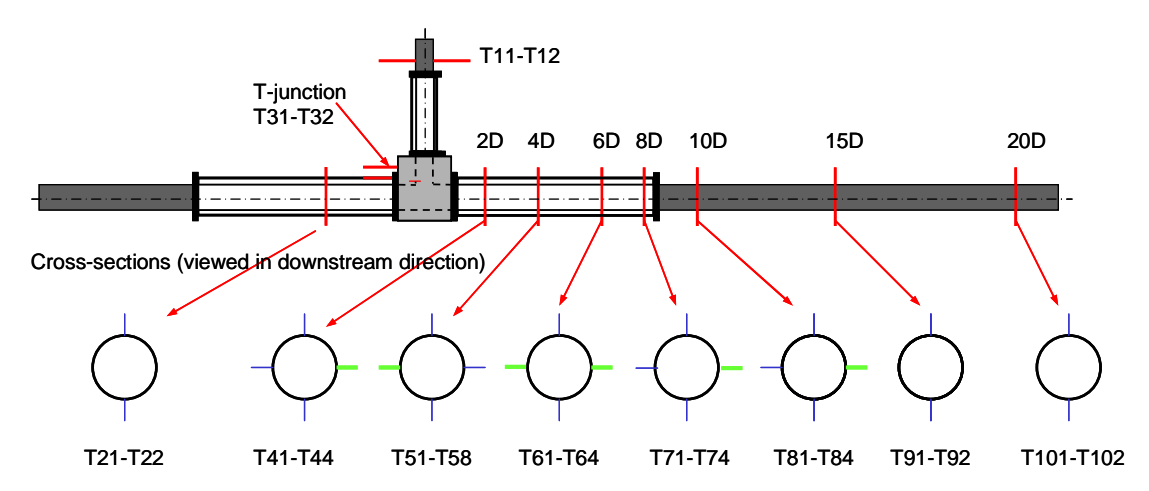


Figure 4. Cross-sections where thermocouple measurement were taken

Temperature fluctuations were recorded using thermocouples (TCs) located 1 mm from the wall at seven stations downstream of the T-junction. The positions of the TCs from the first experiments in 2006 are indicated in Fig. 4. The mean temperature, the temperature fluctuations and the temperature fluctuation spectra were all computed from the data collected. A typical response time for the TCs is 13 ms. This was measured by inserting the thermocouple into a hot-water bath, and defining the response time as the rise time from $0.1\Delta T$ to $0.9\Delta T$, where $\Delta T = T_{\text{hot}} - T_{\text{cold}}$, the temperature difference between the inlet flows. The uncertainty in the mean temperature measurements with thermocouples is estimated to be within ± 0.5 °C [13], which gives a constant uncertainty of 0.03 in terms of the normalised temperature T^* defined by

$$T^* = (T - T_{cold})/\Delta T \tag{1}$$

The statistical uncertainties in $T_{\rm rms}$ are typically less than 3%, except for a few locations near the lower wall where the signal is highly intermittent. However, an additional uncertainty of 5% has to be added to account for possible systematic errors. The total uncertainty in the temperature fluctuations is then estimated to be 8% of the measured value, except near the lower wall, where an uncertainty of 13% has been assumed.

2.3 Inlet Conditions for CFD Computations

The volumetric flow rates used in the benchmark test are given in Table 3, together with the locations where the velocity distributions over the pipe cross-sections were measured (the left and upper red lines in Fig. 3). The temperatures for the cold and hot inlets are also given at these cross-sections. The temperatures of the inflowing streams were assumed to be uniform at the measuring locations, and only one thermocouple was placed there: this appears in the 2nd column of Table 3.

Inlet/designation	Temperature (°C)	Pipe diameter (mm)	Measuring location (mm)#	Volumetric flow rate (litres/s)
Main/InCo	19	140 (D ₂)	-420 (-3D ₂)	9.0
Branch/InHo	36	100 (D ₁)	-310 (-3.1D ₁)	6.0

Table 3: Inlet temperatures and flow rates

The inlet velocity profiles at the upstream stations (Table 3, 4^{th} column) are those taken from an earlier test [13] for which the volumetric flow ratio $Q_2/Q_1 = 2$ rather than the $Q_2/Q_1 = 1.5$ for the benchmark test. Since the flowrate in the hot inlet Q_1 was kept the same (6 l/s), the profiles measured before are also applicable to the present test. The flowrate in the cold inlet is now 9.0 l/s instead of the 12.0 l/s used previously. However, since the velocity profile is fully developed, the profile measured before just need scaling to fit the present flowrate. This exercise was left to the participants.

For the main pipe, the measuring plane is $-3D_2$ upstream from the centre of the T-junction. Mean and rms profiles for the streamwise velocity component are drawn in the left column of Fig. 5 and for the cross-stream components in the right column. The two cross-stream profiles zcl and ycl for the streamwise component U are essentially identical, which is to be expected given that the flow should be axisymmetric; likewise for the cross-stream velocity components V and W. The definitions of the quantities are:

$$U = \overline{u} = \frac{1}{n} \sum_{i=1}^{n} u_{i} \qquad U_{rms} = \left(\overline{(u - \overline{u})^{2}} \right)^{1/2}$$
 (2)

^{*}See Fig. 3 for the origin and orientation of the coordinate system

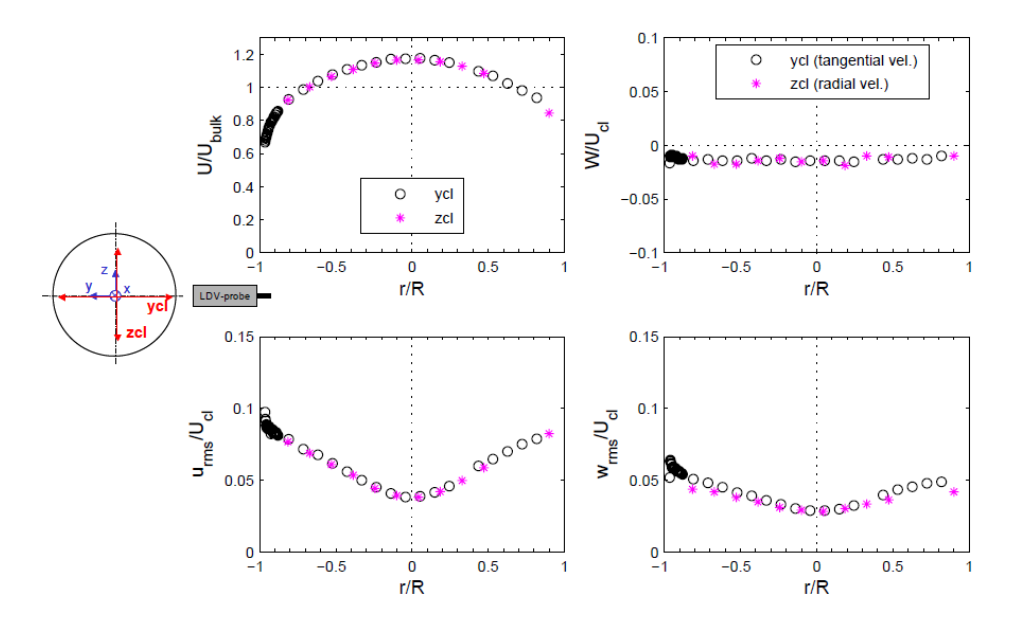


Figure 5. Measured inlet velocity profiles in the cold inlet pipe at $x = -3D_2$: axial (left) and transverse (right)

Figure 6 shows the axial velocity data for the hot water inlet pipe, measured at a cross-section -3.1D₁ upstream of the centre of the T-junction. All profiles indicate a flow with developing boundary layers on the pipe wall, while the central region exhibits characteristics indicating a mainly undisturbed free stream. The centreline velocity is $U_{cl} = 1.11 \times U_{bulk} \approx 0.86$ m/s. Two sets of measurements were carried out: (1) under isothermal conditions, and (2) with hot and cold streams ($\Delta T \approx 15$ K). Both sets of data are included in Fig. 6 and show good correspondence.

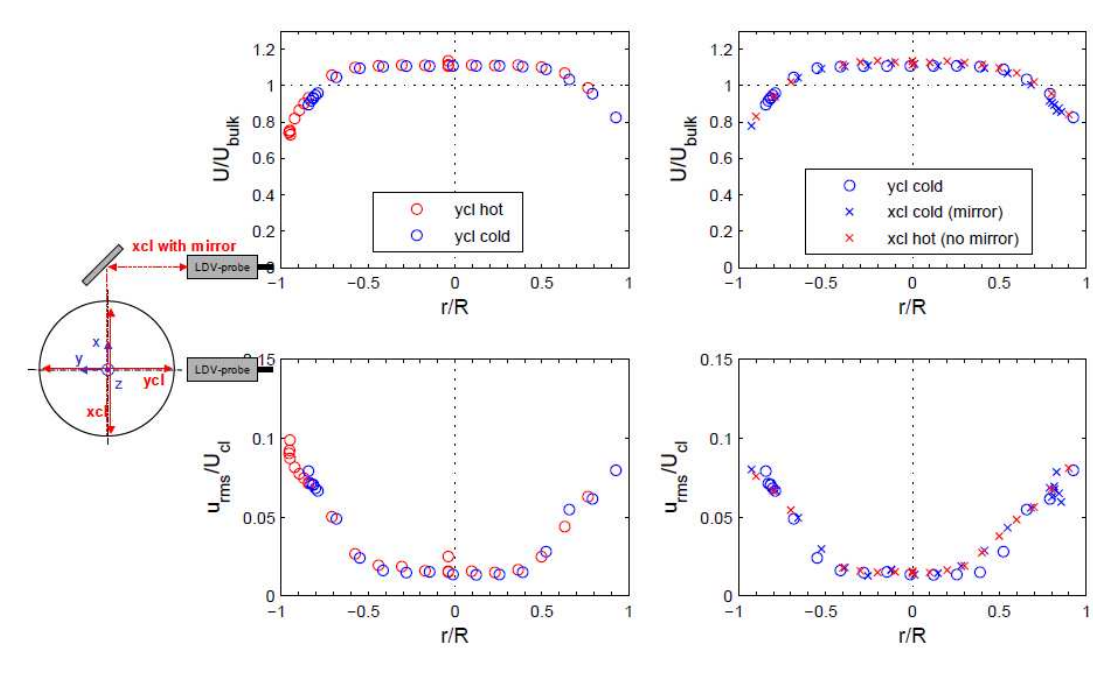


Figure 6. Measured mean and rms axial velocity profiles for the hot inlet at $z = -3.1D_1$ showing that the effects of temperature difference are small

Figure 7 gives the measured mean and rms profiles for the transverse velocity components, again demonstrating the adequacy of performing the velocity measurements under isothermal conditions. The mean velocities are close to zero, reflecting the very careful upstream flow conditioning, while the rms profiles show typical behaviour of a developing flow. For convenience, all data were made available to the benchmark participants in tabular form.

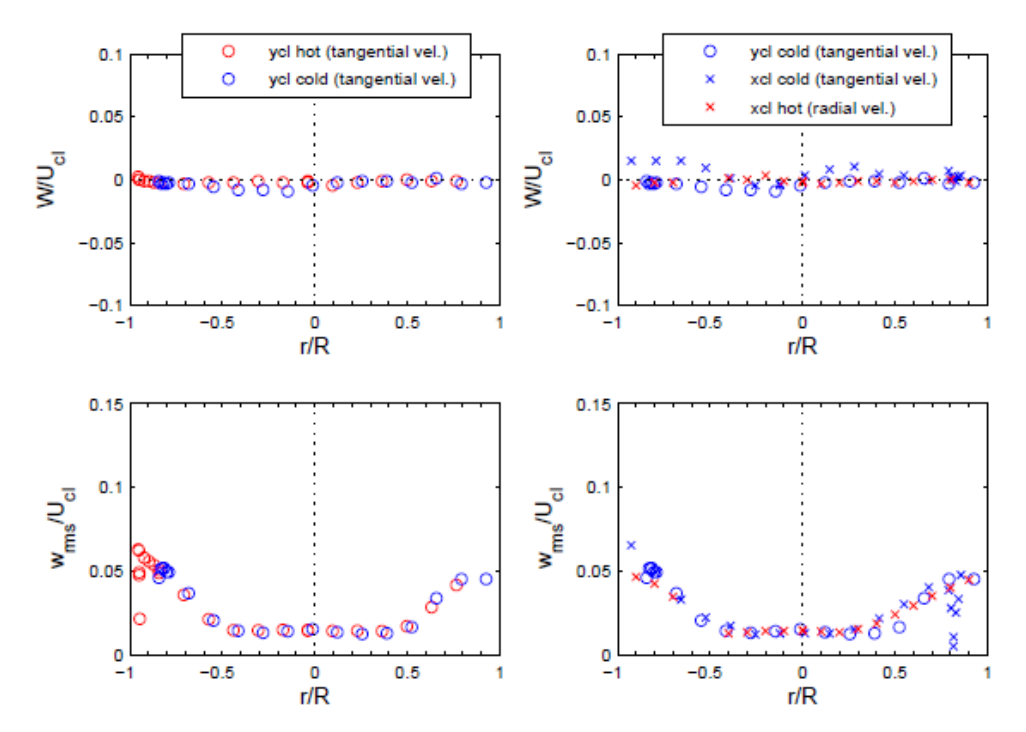


Figure 7. Measured mean and rms transverse velocity profiles for the hot inlet at $z = -3.1D_1$ showing that the effects of temperature difference are small

3. CFD Computations

Participants were deliberately given no clues on how to numerically simulate the test: they were simply requested to provide what they considered to be the most appropriate numerical solution to the problem. Only one submission per registered participant was accepted, and could not be withdrawn once the deadline (April 30, 2009) had passed. Of the 29 sets of results received by the deadline, 8 had been obtained using FLUENT [15], 7 using ANSYS CFX [16], 4 using STAR-CCM+ [17] and 2 using OpenFOAM [18]. Others used in-house CFD codes. For subgrid turbulence, 8 used some form of Smagorinsky, 7 used WALE, 3 used SAS-SST, and the rest used various other models. One code used a Spectral Element (SE) approach, while the rest were Finite Volume (FV). The total discrete number of control volumes ranged from 700 K to over 70 M, with most in the range 1-5 M. Total simulation time ranged between 5 s (minimum requested) to 28 s, with an average of about 10 s. Time-step sizes ranged from 0.06 ms through to 1.0 ms.

Prior to the period of reported data, it was each participant's responsibility to run their simulation for a long enough time interval for time-averaged velocities to become steady. Past simulations of this facility had accomplished this in 2-4 s [13], though it was stipulated that these times served <u>as a guide only</u>. After this initial period, all transient data were to be reported at every 1 ms (a number of participants ignored this stipulation) for at least the last 5 s of the transient calculation, and for no

more than 20 s (to keep the sizes of the results files manageable – though two submissions of 23 s and 28 s exceeded this limit). If time-step sizes other than the 1 ms required for the analysis were used in the calculation, contributors were requested to report their method for data conversion. To characterise the velocity field, all three resolved components of velocity at each measuring position were requested, and the turbulent kinetic energy (k_{SGS}) from the subgrid turbulence model (if available). The number of points along each line segment had to be no less than 20 and no more than 50 for each measuring plane.

To maintain anonymity, each of the 29 submissions is here given a designation S1 to S29, reflecting the chronological order in which they were received. First submission was in January 2010 and the last just a few hours before the cut-off time (Midnight GMT, April 30, 2010).

4. Synthesis of Results

Because of the relatively large number of submissions, an extremely large number of possible comparisons with test data, and between submissions, are possible. As a result, data reduction and plotting were all accomplished using a Python script [19] to minimize the total level of effort. Given the amount of data to be processed, a good starting point was needed for the synthesis of results. A very simple metric was chosen to quickly compare the relative quality of the CFD predictions. For any given curve, the metric is defined as:

$$M = \frac{1}{N} \sum_{i=1}^{N} \left| C_i - D_i \right| \tag{3}$$

where N is the total number of CFD results in the curve, C_i is the i^{th} result from the CFD calculation and D_i is the measured value at the same location. In cases where reported CFD and experimental results were not co-located, a simple linear interpolation was applied to the experimental data to obtain an estimated value at the exact location of the CFD result. As an example, for the time-averaged value of U at $x = 1.6D_2$, z = 0, the above formula is applied for the N = 37 data points \bullet on the profile shown in Fig. 8.

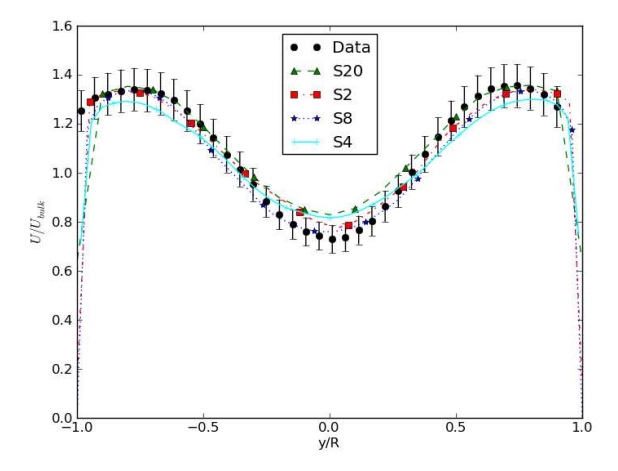


Figure 8. A comparison of the time-averaged U velocity at $x = 1.6D_2$, z = 0 illustrating how the metric (3) is applied

Ranking of submissions was performed separately for the velocity and temperature comparisons. For each application of the metric, the 29 submissions were assigned a rank from 1 (lowest metric value) to 29 (highest metric value). After all comparisons were completed, ranks associated with velocities were summed to provide one summary score, and those associated with temperature were summed for a second summary score. The ranking of the time-averaged *y*-component of velocity, which should be zero due to symmetry, was not included in the final score.

Table 4. Submissions Ranked by Comparisons to PIV Data

Label	Score	Code	Turbulence Model	Cells
S20	75	FLUENT	LES, Dyn. Smagorinsky	70.5M
S2	166	Fluent 12	LES, Dyn. Smagorinsky	34M
S8	178	STAR-CCM+/3.06.006	LES-Wale SGS	13.2 M
S4	184	Fluent 6.3.26	LES, Dyn. Smagorinsky	5.8M
S24	212	OpenFOAM 1.6	LES, Dyn. Smagorinsky	8 M
S21	247	Nek5000	LES, spectral damping	21M
S16	270	Fluent 12	LES-WALE	7.7M
S 3	311	CFX5 v12	LES, WALE	0.97M
S11	312	CFX	LES-Wale	3.4M
S19	322	FLUENT 12.1	SST-kω [#]	11 M
S18	349	CFX	DES-SST	2.4M
S14	358	CABARET	ILES	1.8M
S17	374	OpenFOAM 1.6	LES, 1eqn. Dyn. eddy	0.28M
S 9	375	Advance/FrontFlow/red v4	LES-Smagorinsky	4.1 M
S22	404	STAR-CCM+	LES	4.4 M
S 6	408	STAR-CCM+/3.06.006	LES-Wale	9.3 M
S26	432	FLUENT v12.1	LES - Dynamic KE SGS	7.2 M
S27	446	STAR-CCM+	V^2F	0.62 M
S23	458	CFX	LES-WALE	1.9 M
S10	477	Fluent 12	LES-Smagorinsky-Lilly	0.92M
S25	585	TransAT	LES-WALE	2.5 M
S1	589	Fluent	LES	4.5M
S7	603	CFX	SAS-SST	5.0 M
S15	605	CFX	SAS-SST	2.3M
S13	706	CFX 12.0	SAS-SST	1.1M
S12	712	MODTURC_CLAS	k-epsilon/RNG	0.89M
S29	719	CFX	SAS-SST	1.0M

[#] Slightly modified version of the standard model in which the turbulent viscosity is scaled by a factor 0.38

The final ranking for velocity-based comparisons is shown in Table 4. Two submissions are missing from the Table, due to problems in data formatting discovered too late to be included in the final analysis. The lower the score, the better is the agreement to the measured data. It should be noted that the ranking method used here is just intended as a means of extracting useful summary information from the results, and other metrics could also have been used. The first thing to observe is that the LES approaches fill the top 9 positions in the ranking. Overall, for the same selection of turbulence model, the total number of discrete volumes is generally a good indicator of quality of comparison. In 10^{th} position comes a submission in which the SST-k ω model has been used. This looks impressive, but it should be recalled that 11 M cells were employed, which is excessive for a RANS model. Looking at the entries near the bottom of the Table, it is clear that the SAS-SST model is significantly under-performing in this application.

Table 5. Submissions Ranked by Comparison to Thermocouple Data

Submission	TC Score	Code	Turbulence Model	Volumes
S21	36	Nek5000	LES, spectral damping	21M
S16	45	Fluent 12	LES-WALE	7.7M
S8	48	STAR-CCM+/3.06.006	LES-Wale SGS	13.2 M
S4	57	Fluent 6.3.26	LES, Dyn. Smagorinsky	5.8M
S22	72	Star-CCM+	LES	4.4 M
S23	78	CFX	LES-WALE	1.9 M
S5	81	Saturne	LES, Dyn. Smagorinsky	6.2M
S2	82	FLUENT 12.1	LES, Dyn. Smagorinsky	34M
S20	82	FLUENT	LES, Dyn. Smagorinsky	70.5M
S19	83	FLUENT 12.1	SST-kω	11 M
S14	88	CABARET	ILES	1.8M
S25	88	TransAT	LES-WALE	2.5 M
S18	93	CFX	DES-SST	2.4M
S10	105	Fluent 12	LES-Smagorinsky-Lilly	0.92M
S26	105	FLUENT v12.1	LES - Dynamic KE SGS1	7.2 M
S6	110	STAR-CCM+/3.06.006	LES-Wale	9.3 M
S17	121	OpenFOAM 1.6	LES, 1eqn. Dyn. eddy	0.28M
S7	124	CFX	SAS-SST	5.0 M
S11	138	CFX	LES-Wale	3.4M
S1	139	Fluent	LES	4.5M
S24	151	OpenFOAM 1.6	LES, Dyn. Smagorinsky	8 M
S9	164	Advance/FrontFlow/red v4	LES-Smagorinsky	4.1 M
S15	164	CFX	SAS-SST	2.3M
S13	186	CFX 12.0	SAS-SST	1.1M
S27	186	Star-CCM+	V^2F	0.62 M
S29	197	CFX	SAS-SST	1.0M
S3	201	CFX5 v12	LES, WALE	0.97M
S12	224	MODTURC_CLAS-IST	k-epsilon/RNG	0.89M

The final ranking based on temperature comparisons is shown in Table 5. One submission is missing from the Table, due to late discovery of data reporting errors. Again, LES simulations fill the top 9 positions, but these are not the same as those in Table 4, and the ordering has also changed. In fact, only 7 of the LES submissions appear in the top 10 positions in both the velocity and temperature ranking tables. As before, the SST-kω model is performing well and the SAS-SST model is underperforming, though submission S7, with 5 M volumes, has improved its position in the ranking. Another interesting feature is that submission S20, which employs the most number of cells (>70M), and was ranked #1 in the velocity rankings, drops to #9 in the temperature rankings. In contrast, S21, with the third largest number of cells (~21 M), ranks #2 and #1, respectively. Both are LES simulations, so it appears that the distribution of meshes is crucial, not just the overall number.

A metric based on time-averaged rms error produced rankings and scores very close to those above based upon the magnitude of the mean error. Submissions S3 and S11 swap positions in Table 4, and submissions S19 and S20 swap positions in Table 5. In both instances, the scores only differed by one, so there are no significant changes.

The primary goal of the Fourier analysis was to check the simulations for evidence of periodic low-frequency flow oscillations. A secondary goal was to compare the turbulence spectra predicted by

LES with those derived from the measured data. For a meaningful comparison of amplitudes from the discrete Fourier transforms, all data sets should ideally be of the same time duration, and with the same sampling frequency. This was not possible given the diversity of the data sets involved here. However, by visual inspection of the Fourier transforms of the transient velocity and temperature data at selected measuring points, it was possible to identify a peak in the experimental data near 3.5 Hz. From this same experimental set up, Odemark et al. [13] recorded low-frequency peaks in the temperature data of 3, 4 and 6 Hz for flow ratios $Q_{main}/Q_{branch} = 1$, 2 and 4, respectively. So, a peak around 3.5 Hz for the present case ($Q_{main}/Q_{branch} = 1.5$) was not unexpected.

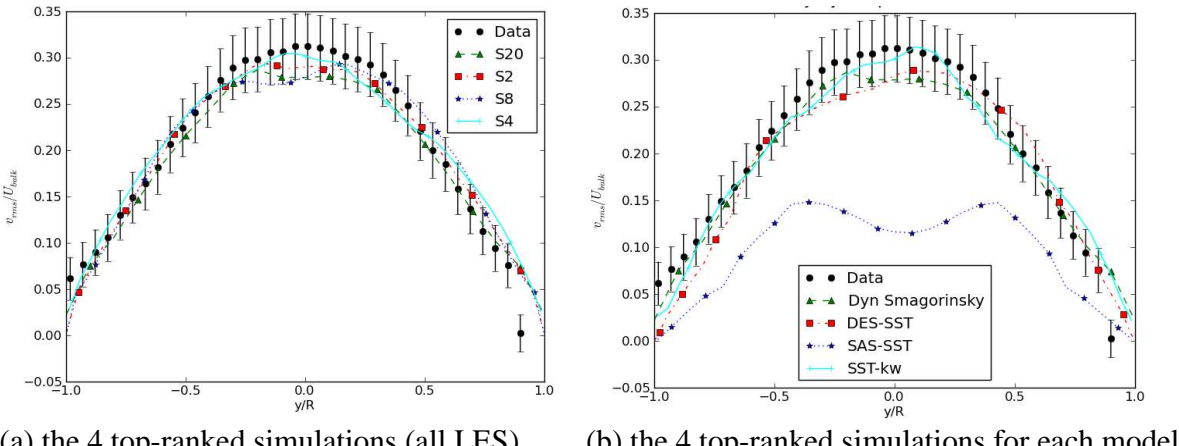
Table 6. Number of Matches of PIV Peaks

Label	PIV Count	Turbulence Model	Duration	Total nodes
S4	27	LES, Dynamic Smagorinsky	15 s	5.8M
S20	23	LES-Dynamic-Smagorinsky	23 s	70.5M
S 8	17	LES-Wale SGS	28 s	13.2M
S18	16	DES-SST	13 s	2.4M
S5	15	LES, Dynamic Smagorinsky	5 s	6.2M
		LES - Dynamic Kinetic Energy		
S26	14	SGS Model	18 s	7.2 M
S6	14	LES-Wale	10 s	9.3 M
S1	13	LES	5 s	4.5M
S17	13	LES, 1eqn. Dynamic eddy	20 s	0.28M
S19	12	SST-kω	10 s	11M
S27	12	V^2F	5 s	0.62 M
S2	11	LES, Dynamic Smagorinsky	20 s	34M
S10	9	LES-Smagorinsky-Lilly	14 s	0.92M
S11	9	LES-Wale	6.9s	3.4M
S24	9	LES-Dynamic-Smagorinsky	5 s	8 M
S25	9	LES-WALE	5.5 s	2.5 M
S16	8	LES-WALE	5.5 s	7.7M
S21	8	LES, spectral damping	5.9 s	21M
S22	7	LES	6.2 s	4.4 M

Some pre-selection of the experimental datasets to be used as the basis of the ranking was necessary, since the 3.5 Hz peak was not always noticeable in the spectra. For instance, only 3 thermocouple readings could be used, while over 30 of the PIV datasets contained a peak at 3.5 Hz. From this subset, a count of matching peaks was made from the spectra of the CFD transient data. Table 6 lists all submissions with more than 5 matches to peaks in the spectra near 3.5 Hz. Submissions employing LES or Detached Eddy Simulation (DES) turbulence models almost fill the table, though SST-kω does quite well. The SAS-SST model appears not to be able to reproduce the spectral peaks, and did not reach the 5 matches criterion to even appear in the Table.

As illustration of the effects of the different modelling approaches, Fig. 9 gives a comparison between measured and numerical profiles of the time-averaged rms values of the vertical velocity v in the horizontal plane z=0 at the first PIV measuring station ($x=1.6D_2$) downstream of the junction. In Fig. 9a, the top four calculations as they are ranked in Table 4 are compared. A comparison of the mean values of U in the same plane is given in Fig. 8 for the same calculations. In all cases, predictions fall within the experimental uncertainty. Figure 9b is a comparison between

different turbulence modelling approaches. In each case, the highest ranked submission according to Table 4 is chosen to represent the particular modelling group: i.e. S20 (LES), S18 (DES), S7 (SAS) and S19 (RANS). Clearly, the SAS-SST model seriously underpredicts the measured profile in terms of absolute value, and has the wrong shape. The other models accurately predict the profile within the experimental uncertainty.



(a) the 4 top-ranked simulations (all LES)

(b) the 4 top-ranked simulations for each model

Figure 9. A comparison of the time-averaged rms fluctuations for v at $x = 1.6D_2$, z = 0

5. **Conclusions**

Within the working group WGAMA of the OECD/NEA, an international blind benchmarking exercise has been conducted to assess the ability of CFD codes to predict turbulent mixing in a Tjunction, an issue of importance in high-cycle thermal fatigue. A very careful mixing experiment had been performed at Vattenfall R&D, Sweden, and provided the data for comparison. Velocity profiles just upstream of the junction were provided and a constant temperature difference $\Delta T = 17$ K was maintained between the branch and main pipes of the tee. Participants were invited to predict velocities and temperatures downstream. In total, there were 65 registrations from groups in 22 countries. Each received the benchmark specifications, and 29 submitted results ahead of the deadline, just prior to release of the test data.

The majority used commercial CFD software (8 used FLUENT, 7 used ANSYS-CFX and 4 used STAR-CCM+), 2 used the open-source software OpenFOAM, while the rest used codes developed in-house. The number of control volumes used varied from 0.28 M to 70.5 M, though most were in the range 1 M to 5 M. The majority (19) chose some variant of Large Eddy Simulation (LES) for the turbulence modelling, others (3) chose Detached Eddy Simulation (DES), while the remainder elected for some form of Reynolds-Averaged Navier Stokes (RANS) model. The time step for advancing the solution ranged from 0.06 ms to 1.0 ms, the average being 0.6 ms. The time for collecting data was set at a minimum of 5 s in the specifications, and 12 participants used this value. One calculation was taken to 28 s, with the average close to 10 s.

There is a mass of data available for analysis, and it is hoped that the participants will explore the possibilities in connection with their own simulations. Only an overall assessment can be given here. Best comparisons with measured data were obtained using LES. For the velocity-based comparisons, for the same selection of turbulence model, the total number of discrete volumes is generally a good indicator of quality of results. This suggests that most participants had been careful in their selection of number of meshes within the constraints of their available computer resources. Also, for roughly the same number of volumes, the SAS-SST appears to be significantly under-performing LES, independently of the sub-grid scale (SGS) model adopted for the latter. Other results show that SST- $k\omega$ in particular is performing quite well, though a large number of meshes (11 M) had been employed in comparison with other RANS submissions.

The submissions were ranked according to three separate metrics. The first was based on the degree of correspondence to the measured velocity data. On this scale, LES approaches occupied the first 9 positions, the SST-kω submission came next, followed by the DES-SST submission. The positions changed somewhat when ranked according to correspondence with the temperature data, but overall LES still occupied the first 9 positions, with SST-kω again in 10th place. Finally, a ranking was made in terms of correspondence of a local peak in the experimental velocity spectra near 3.5 Hz, as had been observed in the experiment, but only at those measurement positions, and for those velocity components, for which a peak was clearly discernible. LES again performed well (though the ordering changed again) filling 7 of the top 8 positions of the ranking table. The DES-SST and SST-kw results were also good, and a RANS simulation (with the v2f model) was considered respectable on the basis of the Fourier metric, even though it performed the worst of all according to the velocity and temperature metrics. The Fourier metric also confirmed the observation made for time-averaged behavior: namely, that SAS-SST had some significant problems with this benchmark, and submissions using this turbulence model did not do well enough matching spectral peaks to even be included in the ranking. Hopefully, some of the participants using this approach will perform follow-up studies to understand the source of the problems and provide guidelines for future use.

Overall, the T-junction benchmark has been very successful. Participation was very high, given that the calculations were extremely demanding in terms of computer time. The exercise complements the activities in other areas in understanding the origins of thermal fatigue in this geometry, and being able to quantify them. Different codes, different modelling approaches, and different numbers of control volumes have been adopted by the various participants, and there is even useful information forthcoming from the modeling options chosen by those who used the same code. Further insights will no doubt be forthcoming from post-test analyses, and a follow-up activity has recently been launched, with organization provided by the European CFD Network, following similar guidelines to those described here. Results from this exercise will appear in due course.

6. References

- [1] "Validation of fast reactor thermomechanical and thermohydraulic codes", IAEA TECDOC-1318, 2002.
- [2] V.N. Shah, *et al.* "Assessment of field experience related to Pressurized Water Reactor primary system leaks", Proc. ASME Pressure Vessel and Piping Conf., Boston, MA, USA, August 1-5, 1999.
- [3] D. Jungclaus, *et al.* "Common IPSN/GRS safety assessment of primary coolant unisolable leak incidents caused by stress cycling", NEA/CSNI Specialist Meeting on Experience with Thermal Fatigue in LWR Piping caused by Mixing and Stratification, OECD/NEA, Paris France, 7-12 June, 1998.

- [4] M. Wakamatsu, H. Nei, K. Hashiguchi, "Attenuation of temperature fluctuations in thermal striping", *J. Nucl. Sci. Tech.*, **32**(8), 752-762 (1995).
- [5] J.I. Lee, P. Saha, M.S. Kazimi, "A parametric study of high cycle thermal fatigue caused by thermal striping,", Proc. 2004 Int. Congress on Advances in Nuclear Power Plants (ICAPP'04), Pittsburgh, PA, USA, June 13-17, 2004.
- [6] L.W. Hu, M.S. Kazimi, "A simplified method for determination of high cycle thermal fluctuations caused by thermal striping", Proc. 2004 Int. Congress on Advances in Nuclear Power Plants (ICAPP'04), Pittsburgh, PA, USA, June 13-17, 2004.
- [7] L.W. Hu, M.S. Kazimi, "Large Eddy Simulation of water coolant thermal striping in a mixing tee junction", Proc. 10th Int. Topical Meeting on Nuclear Reactor Thermal Hydraulics (NURETH-10), Seoul, Korea, Oct. 5-9, 2003.
- [8] C. Faidy, "Thermal fatigue in mixing tees: a step by step simplified procedure," Proc. 11th Int. Conf. on Nuclear Engineering (ICONE-11), Tokyo, Japan, 20-23 Apr., 2003.
- [9] J. Westin, *et al.* "Experiments and unsteady CFD-calculations of thermal mixing in a T-junction", Proc. Benchmarking of CFD Codes for Application to Nuclear Reactor Safety (CFD4NRS), Garching, Germany, 5-7 Sept., 2006 (CD-ROM).
- [10] J. Westin, "Thermal mixing in a T-junction. model tests at Vattenfall Research and Development AB 2006. Boundary conditions and list of available data for CFD-Validations", Vattenfall internal document (private communication), 2007.
- [11] K.-J. Metzner, U. Wilke, "European THERFAT project thermal fatigue evaluation of piping system tee connections", *Nucl. Eng. Des.*, **235**, 473-484 (2005).
- [12] J. Westin, *et al.* "High-cycle thermal fatigue in mixing tees. Large-Eddy Simulations compared to a new validation experiment", Proc. 16th Int. Conf. on Nuclear Engineering (ICONE-16), May 11-15, 2008, Orlando, Florida, USA.
- [13] Y. Odemark, *et al.* "High-cycle thermal fatigue in mixing tees: new Large Eddy Simulations validated against new data obtained by PIV in the Vattenfall experiment", Proc. 17th Int. Conf. on Nuclear Engineering (ICONE-17), July 12-16, 2009, Brussels, Belgium.
- [14] M.V. Zagarola, A.J. Smits, "Mean-Flow Scaling of Turbulent Pipe Flow", *J. Fluid Mech.*, **373**, 33-79 (1998).
- [15] http://www.fluent.com/
- [16] http://www.ansys.com/Products/cfx.asp
- [17] http://www.cd-adapco.com/
- [18] http://www.opencfd.co.uk/openfoam/
- [19] <u>www.python.org</u>